Received: 30 November 2021 | Accepted: 20 January 2022

DOI: 10.1111/1759-7714.14338

ORIGINAL ARTICLE

WILEY

Circ_0010235 facilitates lung cancer development and immune escape by regulating miR-636/PDL1 axis

Jixing Zhao | **Wu Yan** | **Wencong Huang** | **Yongsheng Li**

Department of Thoracic Surgery, Huizhou Central People's Hospital, Huizhou, China

Correspondence
Yongsheng Li, Department of Thoracic Surgery, Huizhou Central People's Hospital, No. 41 North Goose Ling Road, Huicheng District, Huizhou 516001, China.
Email: hzlys1963@163.com

Abstract

Background: Circular RNAs (circRNAs) are a class of important regulators in various human cancers, including lung cancer. Here, we aimed to investigate the role of circ_0010235 in lung cancer.

Methods: The expression of circ_0010235, microRNA-636 (miR-636) and PDL1 was measured by quantitative real-time PCR (qRT-PCR). Cell proliferation was evaluated by CCK-8, colony formation, and 5-ethynyl-2′-deoxyuridine (EdU) assays. Cell apoptosis was detected by flow cytometry. Cell invasion was assessed by transwell assay. All protein levels were determined by western blot assay. In order to detect the roles of circ_0010235 in immune escape, lung cancer cells were cocultured with peripheral blood mononuclear cells (PBMCs) or cytokine-induced killer (CIK) cells in vitro. The relationship between miR-636 and circ_0010235 or PDL1 was verified by dual-luciferase reporter assay and RNA pulldown assay. Immunohistochemistry (IHC) analysis was used to detect Ki67 and programmed death-ligand 1 (PDL1) expression. A xenograft tumor model was established to verify the function of circ_0010235 in vivo.

Results: Circ_0010235 was overexpressed in lung cancer. Circ_0010235 knockdown inhibited proliferation, invasion and immune escape and promoted apoptosis of lung cancer cells. MiR-636 was a target of circ_0010235, and miR-636 inhibition reversed the effects of circ_0010235 knockdown in lung cancer cells. PDL1 was a direct target of miR-636, and miR-636 suppressed the proliferation and invasion and increased apoptosis and antitumor immunity in lung cancer cells by downregulating PDL1. Moreover, circ_0010235 positively regulated PDL1 expression by sponging miR-636. Additionally, circ_0010235 knockdown hampered tumorigenesis in vivo.

Conclusion: Circ_0010235 knockdown inhibited lung cancer progression and increased antitumor immunity by regulating the miR-636/PDL1 axis.

KEYWORDS
antitumor immunity, circ_0010235, lung cancer, miR-636, PDL1

INTRODUCTION

Lung cancer is one of most commonly diagnosed cancers and is the main cause of global cancer-related death.[1,2] Although great therapeutic progress has been achieved over the past few decades, the 5-year survival rate for patients is only 15%.[3] Cytokine-induced killer (CIK) cells are considered as ideal candidate cells for cancer immunotherapy.[4] It has been reported that CIK cells can target many types of tumors and exert their cytotoxic effects after systemic administration.[5] Thus, it is crucial to better clarify the mechanisms of lung cancer development and improve the antitumor immune response of CIK cells.

As a new kind of non-coding RNAs (ncRNAs), circular RNAs (circRNAs) are generated by pre-mRNA back splicing of precursor mRNA and form covalent closed loop structures.[6] Owing to their circular structures, circRNAs can avoid degradation by RNases and have strong stability.[7]

CircRNAs play key roles in regulation of pathological processes and multiple cellular activities.[8,9] Moreover, some circRNAs have been confirmed to be implicated in the development of tumors, including lung cancer.[10–12] Circ_0010235 is located at chr1:19201875-19216599 and is derived from the ALDH4A1 gene. A previous study showed that circ_0010235 acted as a tumor promoter in lung cancer.[13] However, the function of circ_0010235 in lung cancer immune response has not been reported, and its mechanism has not yet been fully established.

Most circRNAs are located in the cytoplasm that can serve as sponges for microRNAs (miRNAs), thus enhancing downstream gene expression by sponging miRNA.[14] MiRNAs are also ncRNAs, acting as critical regulators in the development of tumors via downregulating target gene expression.[15] MiR-636 has been suggested to be implicated in lung cancer progression. However, more roles of miR-636 in lung cancer should be further explored and whether circ_0010235 can modulate lung cancer immune response through the interaction with miR-636 is still unclear. Programmed death-ligand 1 (PDL1; also known as CD274) has been reported to be implicated in tumor immune escape.[16] Moreover, PDL1 has been reported to be upregulated in lung cancer.[17] However, the exact roles of PDL1 in progression of lung cancer and its mechanism remain poorly understood. Coincidently, circ_0010235 and 3′UTR of PDL1 have been found to have a complementary binding sequence for miR-636 by bioinformatic analysis (circinteractome and TargetScan), which prompted us to establish a circ_0010235/ miR-636/ PDL1 regulatory network.

In this study, we examined circ_0010235 expression in lung cancer cells and lung cancer tissues. In addition, we studied the biological function of circ_0010235 in lung cancer progression and antitumor immune response and explored the interactions among circ_0010235, miR-636 and PDL1. The purpose of our study was to provide a promising target for lung cancer diagnosis and treatment.

METHODS

Specimen collection

Lung cancer tissue specimens ($n = 29$) and adjacent normal tissue specimens ($n = 29$) were harvested from non-small cell lung cancer (NSCLC) patients who underwent radical resection surgery at Huizhou Central People's Hospital. Blood samples were obtained from 29 patients with NSCLC and 29 healthy control subjects at Huizhou Central People's Hospital. After collection, tissue specimens were promptly frozen in liquid nitrogen. Blood samples were collected and centrifuged (1600 *g*, 10 min) at room temperature, followed by a second centrifugation (12 000 *g*, 10 min) at 4°C to remove cell debris. Serum supernatant was transferred to a RNase free tube, and then stored in a refrigerator at −80°C until analysis. All subjects had signed their informed consent before recruitment. This study received approval from the Ethics Committee of Huizhou Central People's Hospital.

Cell culture and transfection

Human bronchial epithelial cells (HBE) and lung cancer cell lines (Calu-3, H1650, A549, and H1299) were obtained from COBIOER (Nanjing, China). Calu-3, H1650, A549, and H1299 are NSCLC cell lines. They are all adherent cells with epithelial morphology. RPMI-1640 medium (Invitrogen) including 10% FBS (Sigma-Aldrich) was used to incubate these cells which were maintained under standard conditions (5% CO_2, 37°C).

RiboBio (Guangzhou, China) commercially provided the siRNA against circ_0010235 (si-circ_0010235), circ_0010235-overexpressing vector (circ_0010235), miR-636 mimic (miR-636), miR-636 inhibitor (anti-miR-636), PDL1-overexpressing plasmid (PDL1), and their controls (si-NC, pCD5-ciR, miR-NC, anti-miR-NC, and pcDNA). For cell transfection, A549 and H1299 cells were introduced with the above vector or/and oligonucleotide using lipofectamine 3000 reagent (Invitrogen).

Quantitative real-time PCR (qRT-PCR)

After extracting RNA with Trizol reagent (Invitrogen), reverse transcription was performed using a miRNA reverse transcription PCR kit (for miRNA; RiboBio) or using Primescript RT Reagent (for circRNA/mRNA; TaKaRa). Next, qRT-PCR reaction was manipulated on CFX96Touch system (Bio-Rad) with SYBR Green Master Mix (Roche). Primer information was as follows: circ_0010235 (sense, 5′-CGTCTACCCGGATGAC AAGT-3′; anti-sense, 5′-CTGCGTGAAGGCTAAGACG-3′); ALDH4A1 (sense, 5′-TCTTCCTGAAGGCGGCAGACAT-3′; anti-sense, 5′-GCGTCAATCTCCGCTTGGATCA-3′); miR-636 (sense, 5′-GGGTGTGCTTGCTCGTCC-3′; anti-sense, 5′-CAGTGCGTGTCGTGGAGT-3′); PDL1 (sense, 5′-TGCCGA CTACAAGCGAATTACTG-3′; anti-sense, 5′-CTGCTTGTC CAGATGACTTCGG-3′); GAPDH (sense, 5′-GACTCATGACC ACAGTCCATGC-3′; anti-sense, 5′-AGAGGCAGGGATGAT GTTCTG-3′); U6 (sense, 5′-CTCGCTTCGGCAGCACATAT ACT-3′; anti-sense, 5′-ACGCTTCACGAATTTGCGTGTC-3′). $2^{-\Delta\Delta Ct}$ method was applied for evaluating RNA levels. U6 or GAPDH was used as an endogenous control for detecting miRNA or mRNA/circRNA expression, respectively.

RNase R treatment

Total RNA was treated with RNase R (Seebio) or without RNase R (as negative control) at 37°C for 30 min. Thereafter, the treated RNA was subjected to qRT-PCR for detection of circ_0010235 and ALDH4A1 expression.

Subcellular fraction assay

PARIS Kit (Invitrogen) was utilized to isolate cytoplasm and nucleus fractions. The levels of circ_0010235, U6 (as a nucleus control), and GAPDH (as a cytoplasm control) were assessed via qRT-qPCR.

Cell proliferation assays

Cell counting kit-8 assay was utilized for examining cell viability. Briefly, we seeded transfected (A549 and H1299) cells into a 96-well plate (2000 cells/well). CCK-8 reagent (10 μl, Beyotime,) was placed in each well for 3 h after transfection, followed by detection of the absorbance at 450 nm using a microplate reader (Bio-Rad).

For colony formation assay, we seeded transfected cells (A549 and H1299) into 6-well plates. Fourteen days later, the cells were fixed with methanol (Sangon Biotech) after removing the culture medium. The colonies were imaged and counted after staining with crystal violet (Beyotime).

5-ethynyl-2′-deoxyuridine (EdU) assay was performed using EdU Cell Proliferation Kit (Beyotime) to assess DNA synthesis. In short, transfected cells were inoculated into 24-well plates.Then, 48 h later, we added EdU solution (20 μM) to the each well and they were incubated for 2 h. After fixing in 4% paraformaldehyde, the cells were incubated with 0.5% Triton-X-100, and then stained with Click Additive Solution for 0.5 h. The nucleic acids were stained with DAPI. Finally, EdU positive cells were counted and captured with a fluorescence microscope (Olympus).

Flow cytometry analysis

For cell apoptosis analysis, we seeded the transfected (A549 and H1299) cells into a 6-well plate. After incubation for 48 h, these cells were harvested and then incubated with Annexin V-FITC and PI (Beyotime), followed by measurement of apoptotic cells with FACScan flow cytometer.

Transwell assay

Cell invasive capability was assessed by 24-well transwell inserts (8 μm pore size, Costar, Corning). In brief, the transfected cells were suspended in FBS-free medium and added into the top chamber precoated with Matrigel. Meanwhile, complete medium was added to the bottom chambers (600 μl). Then, 24 h later, cells that had invaded to the bottom surface of the chamber were fixed using methanol (Sangon Biotech). After staining with crystal violet (Beyotime), the images were captured under a microscope (Olympus) at × 100 magnification.

Western blot assay

For extraction of protein, RIPA lysis buffer (Keygen) was used to lyse cells or tissues. After measuring the protein concentration using a BCA protein assay kit (Abcam), electrophoresis was performed with SDS-PAGE to separate the protein. Next, the protein was transferred onto PVDF membranes (Invitrogen), followed by blocking in nonfat milk (5%; Beyotime). After that, the membranes were probed with primary antibodies (overnight, 4°C). The primary antibodies containing Cyclin D1 (1:1000, ab226977), MMP9 (1:2000, ab76003), PDL1 (1:1000, ab205921) and GAPDH (1:2000, ab9485) were all provided by Abcam. After incubation with secondary antibody (1:3000, ab205718, Abcam), enhanced chemiluminescence reagent (Abcam) was used to visualize the blot signal.

CIK cells preparation

Peripheral blood was used from patients being treated with heparin as an anticoagulant. As previously described, Ficoll gradient centrifugation was used to separate the peripheral blood mononuclear cells (PBMCs).[18] We seeded PBMCs into a 6-well plate and PBMCs were cultured in RPMI 1640 containing 1000 U/ml recombinant human interferon-γ (IFN-γ; Boehringer Ingelheim), 1000 U/ml recombinant human interleukin 2 (IL-2; Peprotech), 10% FBS (Invitrogen), 25 mmol/l HEPES (Sigma-Aldrich), and 2 mmol/l L-glutamine (Sigma-Aldrich). Then, 24 h later, monoclonal antibody against CD3 (100 μg/l, BD Bioscience) and interleukin-1 alpha (100 U/ml, Life Technologies) were added. CIK cells were harvested on day 13.

Enzyme-linked immunosorbent assay (ELISA)

ELISA was performed to examine the levels of IFN-γ and TNF-α in cell supernatant. We subsequently collected the cell culture supernatant via centrifugation (1000 × *g*, 10 min, 4°C). Thereafter, the concentrations of FN-γ and TNF-α were examined via ELISA (Abcam).

Cytotoxicity analysis

A549 and H1299 cells served as the target cells, and the effector cells were CIK cells. In this research, the effector and target cells were cocultured at a ratio of 15:1. Target and effector cells acted as controls. These cells were inoculated in a 96-well plate and maintained under standard conditions (5% CO_2, 37°C) for 24 h. After that, CCK-8 (10 μl, Beyotime) was introduced per well and then incubated for another 3 h, followed by detection of the absorbance using a microplate reader (Bio-Rad) at 450 nm. Survival (%) = (effector target cell mixture-effector group)/target cells × 100.

Dual-luciferase reporter assay

Circinteractome or TargetScan was used to predict the interaction between miR-636 and circ_0010235 or PDL1. The fragments of circ_0010235 or PDL1 including the predicated complementary sites of miR-636 were synthesized and inserted into pmirGLO vector (YouBia) to construct wild-type reporter plasmids (WT-circ_0010235 and PDL1

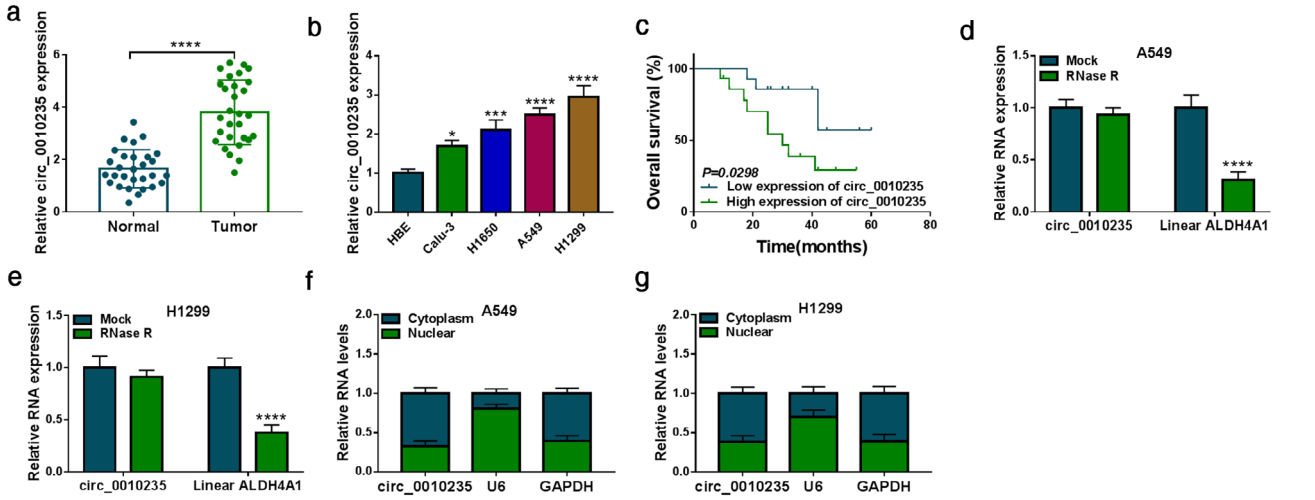

FIGURE 1 Circ_0010235 was overexpressed in lung cancer tissues and cells. (a and b) The expression of circ_0010235 was determined by qRT-PCR in normal tissues, tumor tissues, HBE cells, and lung cancer cells (Calu-3, H1650, A549, and H1299). (c) The survival rate was analyzed between low and high expression of circ_0010235 groups in lung cancer patients. (d and e) The levels of circ_0010235 and ALDH4A1 mRNA were examined after treatment of RNase R by qRT-PCR in A549 and H1299 cells. (f and g) The subcellular location of circ_0010235 in A549 and H1299 cells was examined by qRT-PCR. $^{*}p < 0.05$, $^{***}p < 0.001$, $^{****}p < 0.0001$

3′UTR-WT). Meanwhile, their mutant reporter plasmids (MUT-circ_0010235 and PDL13'UTR-MUT) without miR-636 binding sites were generated as described above. Afterwards, the constructed reporter vector and miR-636/miR-NC were cointroduced into the A549 and H1299 cells. After being incubated for 48 h, dual luciferase reporter gene assay kit (LMAI Bio) was employed for measuring the luciferase activity.

RNA pulldown assay

Biotinylated negative control (bio-miR-NC) and biotinylated miR-636 (bio-miR-636) were commercially provided by RiboBio and introduced into A549 and H1299 cells for 24 h. After that, cells were subjected to RIP lysis buffer, and the cell extracts were treated with M-280 streptavidin magnetic beads (Invitrogen). The RNAs attached to the beads were purified using TRIzol reagent (Invitrogen). Lastly, RNA levels were tested via qRT-PCR after RNA isolation from the magnetic beads.

Immunohistochemistry (IHC)

After fixing with formaldehyde (10%), tumor tissues were embedded in paraffin, and cut into 4-μm thick sections. After incubation with the primary antibody Ki67 (ab15580; 1:200; Abcam) or PDL1 (ab205921; 1:500; Abcam), all sections were further probed with secondary antibody (ab171870, 1:2000, Abcam). Following staining with diaminoaniline (DAB; Sangon Biotech) and counterstaining with hematoxylin (Sangon Biotech), the sections were observed using an Olympus microscope.

TABLE 1 Relationship between circ_0010235 expression and clinicopathological features of lung cancer patients

		circ_0010235 expression		
	Characteristics $n = 29$	**Low ($n = 14$)**	**High ($n = 15$)**	***p*-value[a]**
Gender				0.7104
Female	11	6	5	
Male	18	8	10	
Age (years)				0.6999
≤60	9	5	4	
>60	20	9	11	
TNM grade				0.0253*
I + II	12	9	3	
III + IV	17	5	12	
Lymph node metastasis				0.0268*
Positive	15	4	11	
Negative	14	10	4	
Tumor size				0.0209*
≤5 cm	10	8	2	
>5 cm	19	6	13	

Abbreviation: TNM, tumor-node-metastasis.
[a]Chi-square test.
$^{*}p < 0.05$.

Tumor formation assay in vivo

The following study was approved by the Animal Care and Use Committee of Huizhou Central People's Hospital. Lentivirus packaged plasmid sh-circ_0010235 and

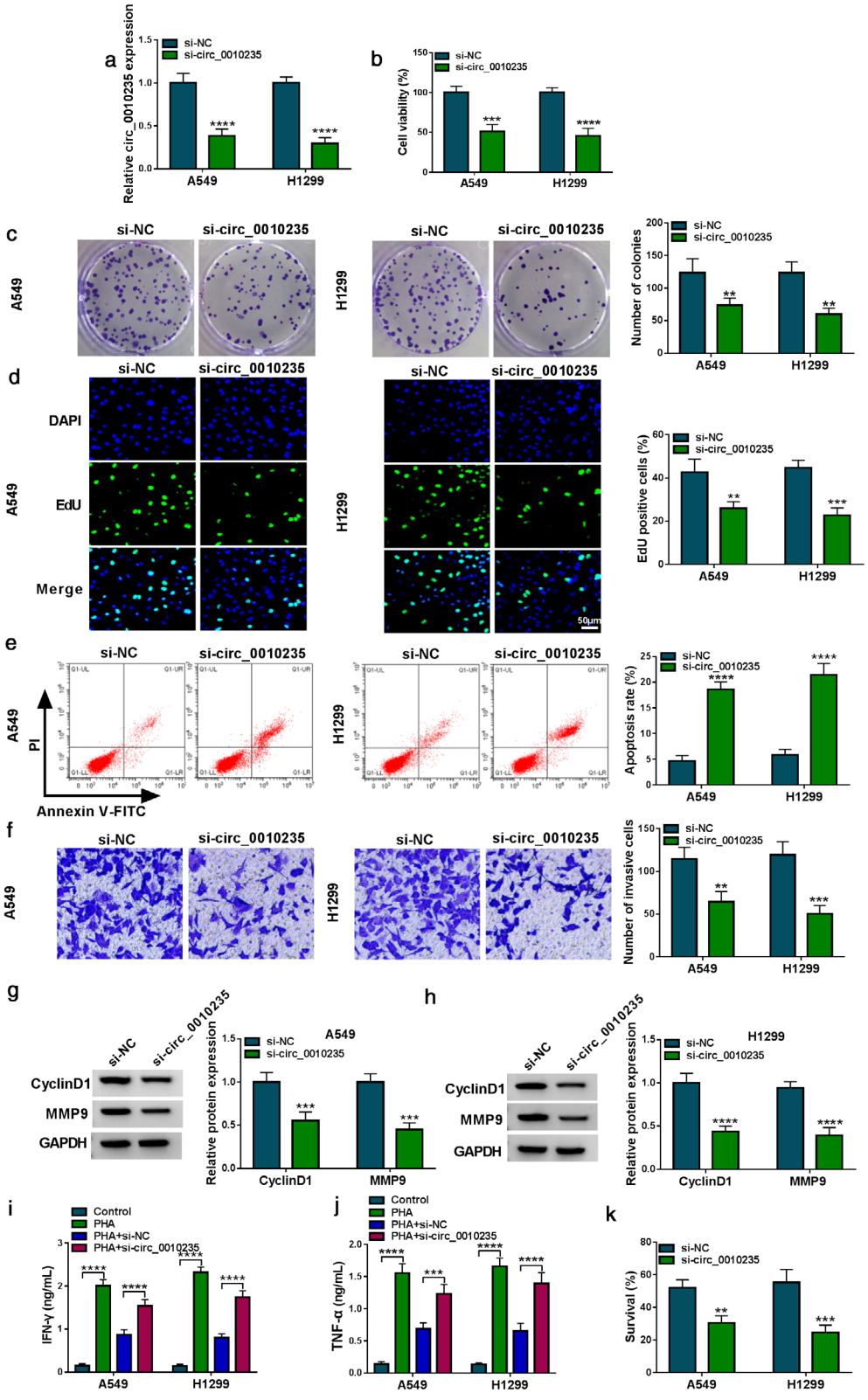

FIGURE 2 Circ_0010235 downregulation inhibited lung cancer cell progression and increased antitumor immune response. A549 and H1299 cells were transfected with si-NC or si-circ_0010235. (a) The expression of circ_0010235 was detected by qRT-PCR. (b) CCK-8 assay was used to detect cell viability. (c) Colony formation assay was performed to examine the number of colonies. (d) DNA synthesis was determined by EdU assay. (e) Flow cytometry analysis was used to examine cell apoptosis rate. (f) Transwell assay was conducted to estimate cell invasion (×100). (g and h) Western blot assay was conducted to measure the protein levels of CyclinD1 and MMP9. (i and j) IFN-γ and TNF-α levels was detected by ELISA in PHA induced PBMCs cocultured with A549 and H1299 cells transfected with si-NC or si-circ_0010235. (k) The survival rate of A549 and H1299 cells was detected by CCK-8 assay when effector-target ratio was 15:1. $^{**}p < 0.01$, $^{***}p < 0.001$, $^{****}p < 0.0001$

sh-NC (as a control) were constructed by RiboBio. BALB/c nude mice (5 weeks, male, $n = 12$) were commercially provided by Vital River (Beijing, China) and randomly divided into two groups (6 mice per group). Briefly, A549 cells (1×10^6, control or circ_0010235 silencing) were inoculated into nude mice. Seven days later, tumor volume of subcutaneous tumors was gauged every three days and calculated using the equation: length × width^2 × 1/2. Twenty-two days later, the mice were killed for subsequent analysis.

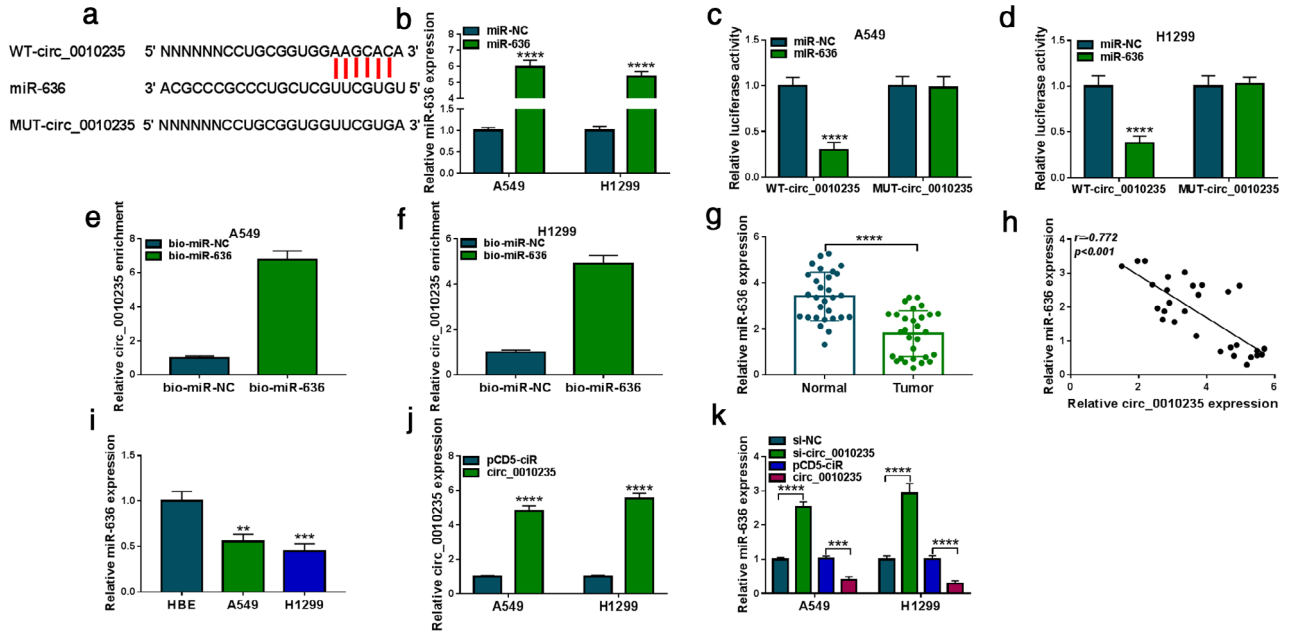

FIGURE 3 MiR-636 was a direct target of circ_0010235. (a) The binding sites between miR-636 and circ_0010235 were predicted by circinteractome. (b) The expression of circ_0010235 was measured by qRT-PCR in A549 and H1299 cells transfected with miR-NC or miR-636. (c and d) Dual-luciferase reporter assay was conducted to measure the luciferase activity in A549 and H1299 cells cotransfected with WT-circ_0010235 or MUT-circ_0010235 and miR-636 or miR-NC. (e and f) Circ_0010235 enrichment was detected by RNA pulldown assay in in A549 and H1299 cells transfected with bio-miR-NC or bio-miR-636. (g) The expression of miR-636 in normal and tumor tissues was detected by qRT-PCR. (h) The correlation between miR-636 and circ_0010235 expression in tumor tissues was analyzed by Pearson's correlation coefficient. (i) MiR-636 expression was examined by qRT-PCR in HBE, A549 and H1299 cells. (j) Circ_0010235 expression was detected by qRT-PCR in A549 and H1299 cells transfected with pCD5-ciR or circ_0010235. (k) The expression of miR-636 was tested by qRT-PCR in A549 and H1299 cells transfected with si-NC, si-circ_0010235, pCD5-ciR, or circ_0010235. $^{**}p < 0.01$, $^{***}p < 0.001$, $^{****}p < 0.0001$

Statistical analysis

All data from at least three independent experiments were analyzed by Graphpad Prism and are shown as the mean ± standard deviation. The difference was compared by Student's *t*-test (two groups) or a one-way analysis of variance (ANOVA; mutiple groups). Survival curve was analyzed by Kaplan–Meier method. The correlation between miR-636 and circ_0010235 or PDL1 in tumor tissues was analyzed with Pearson's correlation coefficient. $p < 0.05$ was considered statistically significant.

RESULTS

Expression level of circ_0010235 was increased in lung cancer tissues and cells

A qRT-PCR was performed in order to determine circ_0010235 expression in lung cancer issues and cells. As shown in Figure 1a, circ_0010235 expression was increased in lung cancer tissues compared with normal tissues. Moreover, the relationship between circ_0010235 expression and clinicopathological features of lung cancer patients was analyzed. We found that circ_0010235 expression was significantly associated with tumor-node-metastasis (TNM) grade, lymph node metastasis, and tumor size, but not with gender and age (Table 1). Similarly, circ_0010235 expression was also enhanced in lung cancer cells (Calu-3, H1650, A549, and H1299) relative to HBE cells, especially in A549 and H1299 cells (Figure 1b). In addition, the lung cancer patients were classified into low expression of circ_0010235 ($n = 14$) and high expression of circ_0010235 ($n = 15$) groups according to the median value of circ_0010235 expression. Patients in the high expression of circ_0010235 group showed poor survival compared with the low expression of circ_0010235 group (Figure 1c). Moreover, the expression of circ_0010235 was higher in serum samples of lung cancer patients than that in healthy volunteers (Figure S1a). Relative operating characteristic (ROC) curves were applied to assess whether circ_0010235 could be used as a potential biomarker. The data showed that serum circ_0010235 could discriminate the lung cancer patients from the healthy controls with relatively satisfactory accuracy, and the AUC value was 0.9126 (Figure S1b). RNase R is an exoribonuclease that can degrade RNA from its 3′ to 5′ end, but does not act on circRNA. As expected, circ_0010235 was resistant to RNase R treatment in contrast to linear ALDH4A1 mRNA (Figure 1d,e). Moreover, circ_0010235 was found to be primarily located in the cytoplasm (Figure 1f,g). Taken together, as a circular RNA, circ_0010235 might be involved in lung cancer progression.

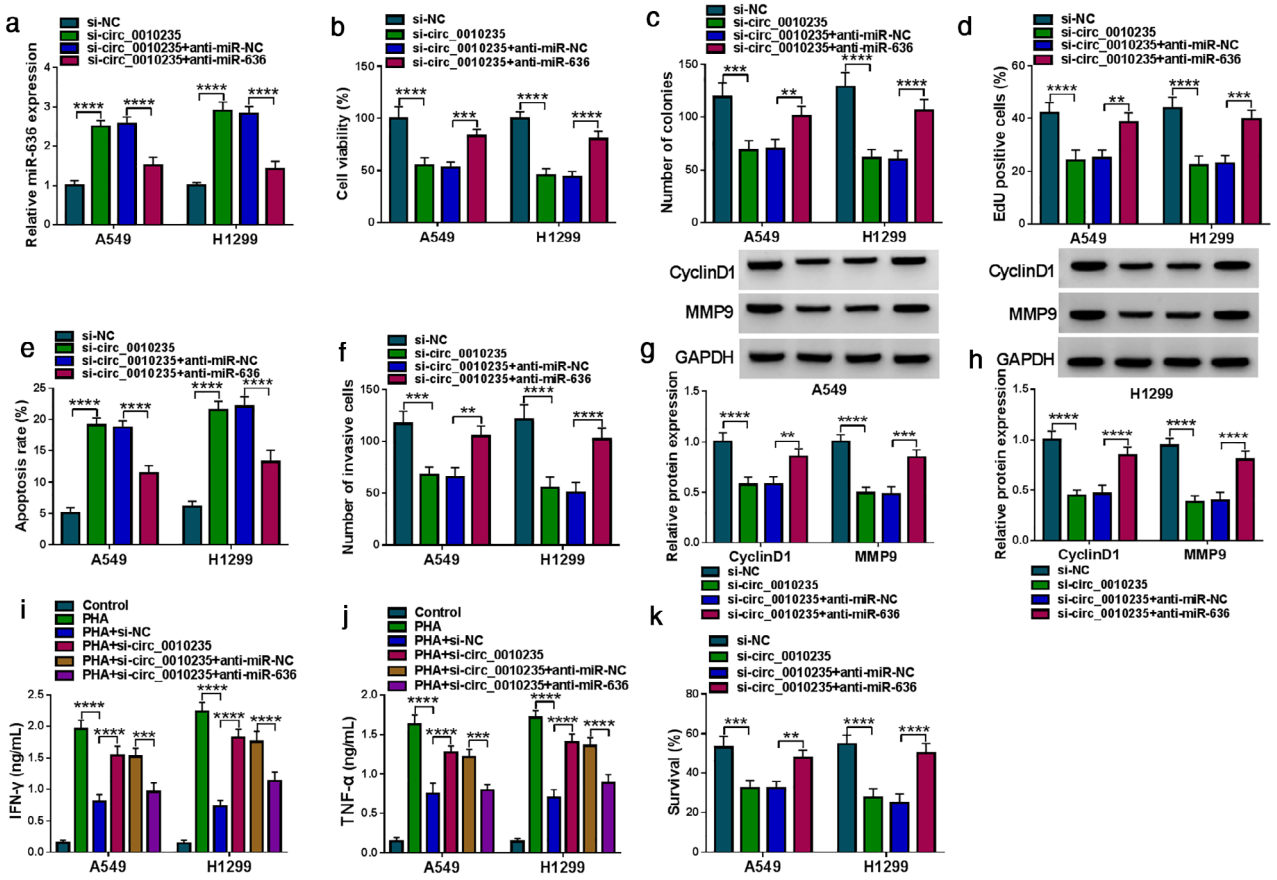

FIGURE 4 Circ_0010235 regulated the proliferation, apoptosis, invasion, and antitumor immunity in lung cancer cells by sponging miR-636. A549 and H1299 cells were transfected with si-NC, si-circ_0010235, si-circ_0010235 + anti-miR-NC, or si-circ_0010235 + anti-miR-636. (a) The level of miR-636 was determined by qRT-PCR. (b–d) CCK-8 assay, colony formation assay, and EdU assay were utilized to evaluate proliferation ability. (e) Flow cytometry analysis was used for detecting cell apoptosis. (f) Cell invasion was determined by transwell assay. (g and h) The protein levels of cyclin D1 and MMP9 were measured by western blot assay. (i and j) IFN-γ and TNF-α levels was examined using ELISA in PHA induced PBMCs cocultured with A549 and H1299 cells transfected with si-NC, si-circ_0010235, si-circ_0010235 + anti-miR-NC, or si-circ_0010235 + anti-miR-636. (k) The survival rate of A549 and H1299 cells was detected via CCK-8 assay when effector-target ratio was 15:1. $^{**}p < 0.01$, $^{***}p < 0.001$, $^{****}p < 0.0001$

Knockdown of circ_0010235 inhibited the proliferation, invasion and immune escape and promoted apoptosis of lung cancer cells

To investigate the role of circ_0010235 in lung cancer, si-NC or si-circ_0010235 was transfected into A549 and H1299 cells. Transfection of si-circ_0010235 successfully knocked down circ_0010235 expression in A549 and H1299 cells (Figure 2a). CCK-8, colony formation, and EdU assays showed that circ_0010235 knockdown suppressed cell viability, colony formation ability, and DNA synthesis in A549 and H1299 cells, indicating that circ_0010235 knockdown inhibited cell proliferation (Figure 2b–d). Flow cytometry analysis suggested that circ_0010235 downregulation induced A549 and H1299 cell apoptosis (Figure 2e). Transwell assay indicated that A549 and H1299 cell invasion were inhibited by circ_0010235 silencing (Figure 2f). Western blot assay showed that circ_0010235 interference inhibited CyclinD1 (a growth-promoting protein) and MMP9 (an indispensable cytokine for cancer cell invasion) protein expression (Figure 2g,h). Next, we explored the effect of circ_0010235 on antitumor immune response. PBMCs were stimulated with phytohemoagglutinin (PHA; Sigma-Aldrich), and then PHA-stimulated PBMCs were cocultured with A549 and H1299 cells transfected with si-NC or si-circ_0010235. We found that IFN-γ and TNF-α levels were increased in PBMCs stimulated with PHA, suggesting enhancement antitumor immunity (Figure 2i,j). In the coculture model, knockdown of circ_0010235 elevated IFN-γ and TNF-α levels (Figure 2i,j), indicating that circ_0010235 downregulation enhanced antitumor immune response via increase of IFN-γ and TNF-α. Subsequently, we analyzed the cytotoxicity of CIK cells on both A549 and H1299 cells when the effector-target ratio was 15:1. We found that circ_0010235 knockdown suppressed A549 and H1299 cell survival rate (Figure 2k), implying that the cytotoxic activity of the CIK cells against circ_0010235-downregulaitng A549 and H1299 cells was markedly higher than that of A549 and H1299 cells transfected with si-NC. These data suggested that circ_0010235 knockdown suppressed lung cancer cell proliferation and invasion increased apoptosis and antitumor immune response.

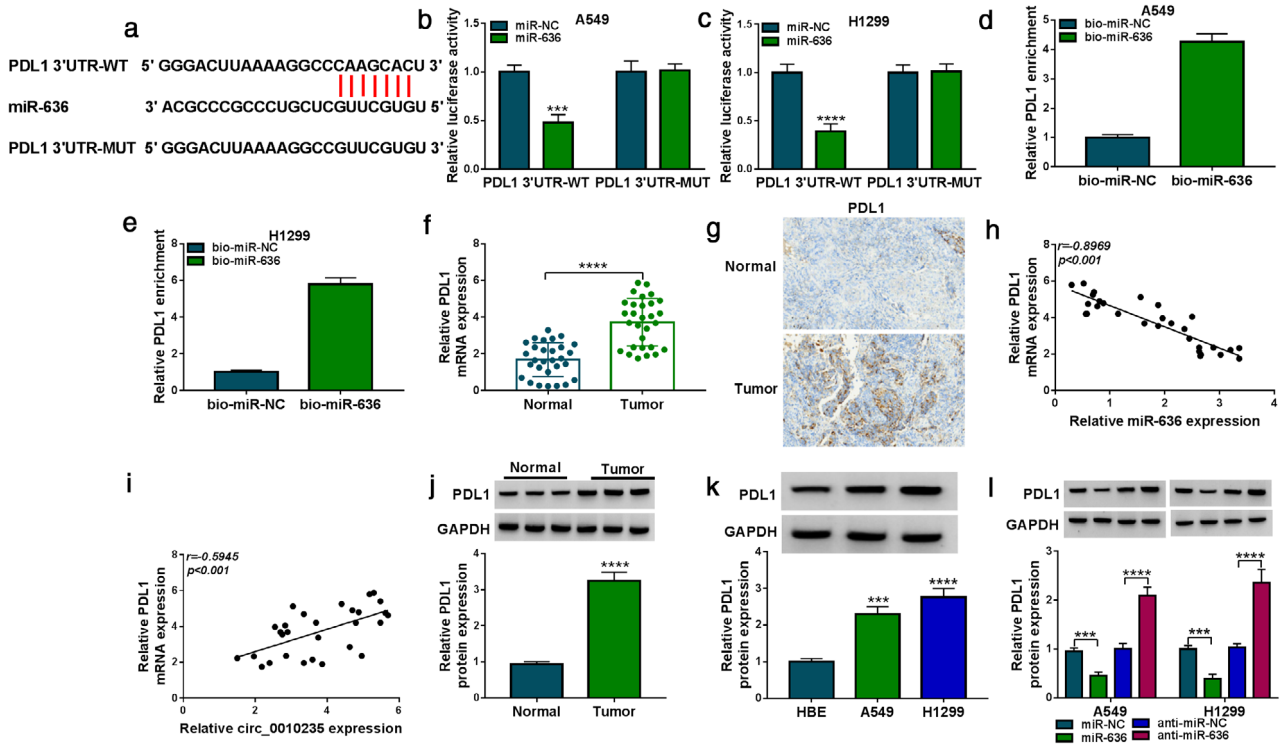

FIGURE 5 PDL1 was targeted by miR-636. (a) The potential binding sites between PDL1 3'UTR and miR-636 were predicted by TargetScan. (b–e) The interaction between miR-636 and PDL1 was confirmed by dual-luciferase reporter assay and RNA pulldown in A549 and H1299 cells. (f) PDL1 mRNA level in normal and tumor tissues was determined by qRT-PCR. (g) PDL1 expression was analyzed in tumor or normal tissues by IHC analysis. (h and i) The correlation between PDL1 and miR-636 or circ_0010235 expression in tumor tissues was analyzed. (j and k) Western blot was carried out to detect the protein expression of PDL1 in normal tissues, tumor tissues, HBE cells, A549 cells, and H1299 cells. (l) PDL1 protein expression was analyzed by western blot assay A549 and H1299 cells transfected with miR-NC, miR-636, anti-miR-NC, or anti-miR-636. ***$p < 0.001$, ****$p < 0.0001$

Circ_0010235 directly interacted with miR-636

Previous studies have indicated that circRNAs can serve as sponges of miRNAs in the cytoplasm of cells.[19] To explore whether circ_0010235 could function as a sponge of miRNA, the potential targets of circ_0010235 were predicted by circinteractome. As presented Figure 3a, there were binding sites between miR-636 and circ_0010235, indicating miR-636 might be a target of circ_0010235. Overexpression efficiency of miR-636 was confirmed by qRT-PCR in A549 and H1299 cells transfected with miR-636 or miR-NC (Figure 3b). To confirm the interaction between miR-636 and circ_0010235, dual-luciferase reporter assay and RNA pulldown assay were performed. The data showed that miR-636 upregulation showed a dramatic suppression in luciferase activity of WT-circ_0010235 but not MUT-circ_0010235 (Figure 3c,d). Furthermore, the enrichment of circ_0010235 was markedly increased in the bio-miR-miR-636 probe (Figure 3e,f). Next, we explored miR-636 expression in lung cancer tissues. miR-636 expression was reduced in lung cancer tissues relative to normal tissues (Figure 3g). An inverse correlation between miR-636 and circ_0010235 expression was found in lung cancer tissues (Figure 3h). Likewise, miR-636 expression in lung cancer cells (A549 and H1299) was lower than that in HBE cells (Figure 3i). Transfection of circ_0010235 increased circ_0010235 expression in A549 and H1299 cells (Figure 3j), indicating a high transfection efficiency. Additionally, overexpression of circ_0010235 decreased the level of miR-636 in A549 and H1299 cells, and knockdown of circ_0010235 displayed an opposite effect (Figure 3k). All these data indicated that miR-636 was sponged by circ_0010235.

MiR-636 inhibition reversed the effects of si-circ_0010235 on proliferation, apoptosis, invasion, and antitumor immunity in lung cancer cells

Based on the above results, we further investigated whether circ_0010235 could regulate lung cancer cell behavior by targeting miR-636. As shown in Figure 4a, miR-636 downregulation reversed si-circ_0010235-induced upregulation of miR-636 in A549 and H1299 cells. In addition, the inhibitory effects of circ_0010235 knockdown on cell viability, colony formation ability, and DNA synthesis were abolished by miR-636 inhibition (Figure 4b–d). Moreover, the proapoptosis and anti-invasion effects caused by si-circ_0010235 were abated by downregulating miR-636 (Figure 4e,f). Meanwhile, the inhibitory effect of circ_0010235 silencing on CyclinD1 and MMP9 protein levels was neutralized by decreasing miR-636 (Figure 4g,h). Furthermore, the enhancement of IFN-γ and

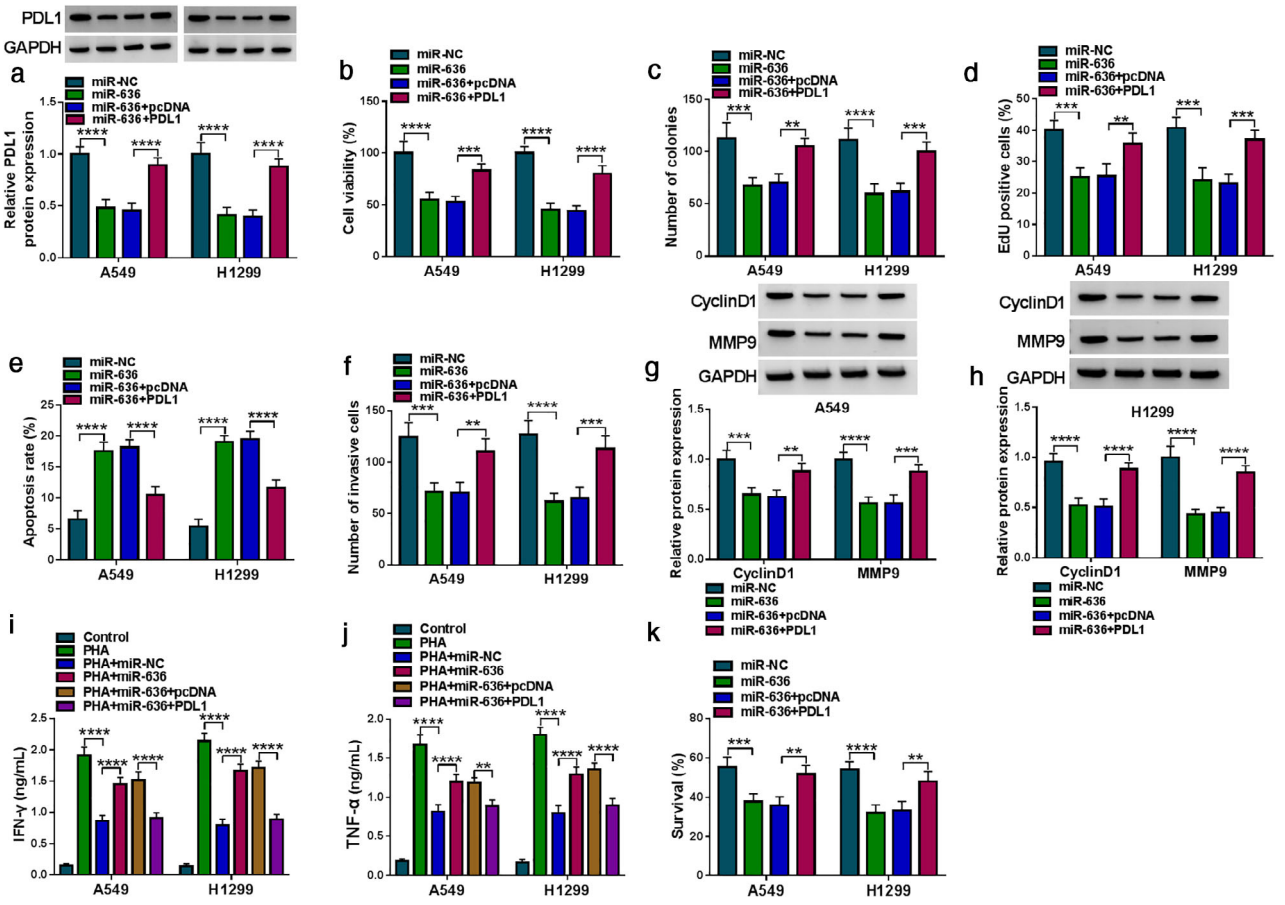

FIGURE 6 MiR-636 exerted an anticancer role in lung cancer cells by targeting PDL1. A549 and H1299 cells were transfected with miR-NC, miR-636, miR-636 + pcDNA, or miR-636 + PDL1. (a) PDL1 protein expression was examined by western blot assay. (b–d) Cell proliferation was assessed using CCK-8, colony formation, and EdU assays. (e) Cell apoptosis was measured using flow cytometry analysis. (f) Transwell assay was used for measuring cell invasion ability. (g and h) Cyclin D1 and MMP9 protein levels were detected by western blot assay. (i and j) ELISA was used to detect IFN-γ and TNF-α levels in PHA induced PBMCs cocultured with A549 and H1299 cells transfected with miR-NC, miR-636, miR-636 + pcDNA, or miR-636 + PDL1. (k) CCK-8 assay was applied to measure the survival rate of A549 and H1299 cells when effector-target ratio was 15:1. $^{**}p < 0.01$, $^{***}p < 0.001$, $^{****}p < 0.0001$

TNF-α levels and the reduction of survival rate caused by circ_0010235 downregulation were counteracted by miR-636 inhibition (Figure 4i,k). Taken together, these data suggested that circ_0010235 knockdown inhibited lung cancer cell progression and increased antitumor immunity by sponging miR-636.

PDL1 was a direct target of miR-636

To identify the underlying mechanism of miR-636, bioinformatic analysis (Targetscan) was performed and we found that PDL1 3′UTR contained binding sites for miR-636 (Figure 5a). The results of dual-luciferase reporter assay suggested that overexpression of miR-636 suppressed the luciferase activity of PDL13′UTR-WT, which could not be observed in PDL1 3′UTR-MUT group (Figure 5b,c). Meanwhile, transfection of bio-miR636 increased PDL1 enrichment compared to transfection of bio-miR-NC in A549 and H1299 cells (Figure 5d,e), confirming the interaction between miR-636 and PDL13. The mRNA level of PDL1 was increased in lung cancer tissues relative to normal tissues (Figure 5f). IHC analysis showed that PDL1 expression was increased in lung cancer tissues compared to normal tissues (Figure 5g). Moreover, we found that PDL1 mRNA expression had a negative correlation with miR-636 expression and had a positive correlation with circ_0010235 expression in lung cancer tissues (Figure 5h,i). Furthermore, PDL1 protein expression was also upregulated in both lung cancer tissues and cells (Figure 5j,k). In addition, the protein expression of PDL1 was reduced by overexpression of miR-636 and increased by inhibiting miR-636 in A549 and H1299 cells (Figure 5l). These outcomes suggested that miR-636 directly targeted PDL1.

MiR-636 suppressed the proliferation and invasion and increased apoptosis and antitumor immunity in lung cancer cells by targeting PDL1

To explore whether PDL1 was involved in miR-636-mediated biological functions in lung cancer cells, rescue assays were performed. Overexpression of PDL1 revealed a reduction of

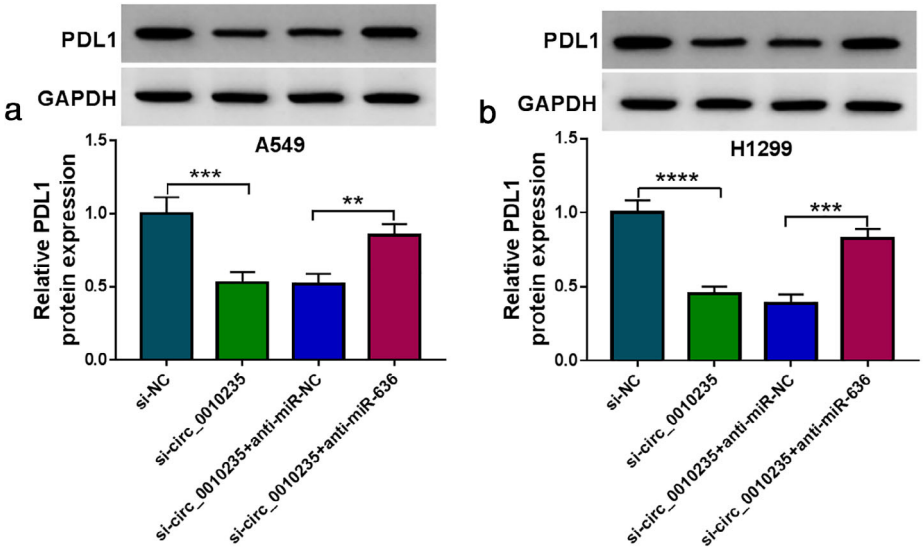

FIGURE 7 Circ_0010235 sponged miR-636 to regulate PDL1 expression. (a and b) Western blot assay was carried out to measure the protein expression of PDL1 in A549 and H1299 cells transfected with si-NC, si-circ_0010235, si-circ_0010235 + anti-miR-NC, or si-circ_0010235 + anti-miR-636. $^{**}p < 0.01$, $^{***}p < 0.001$, $^{****}p < 0.0001$

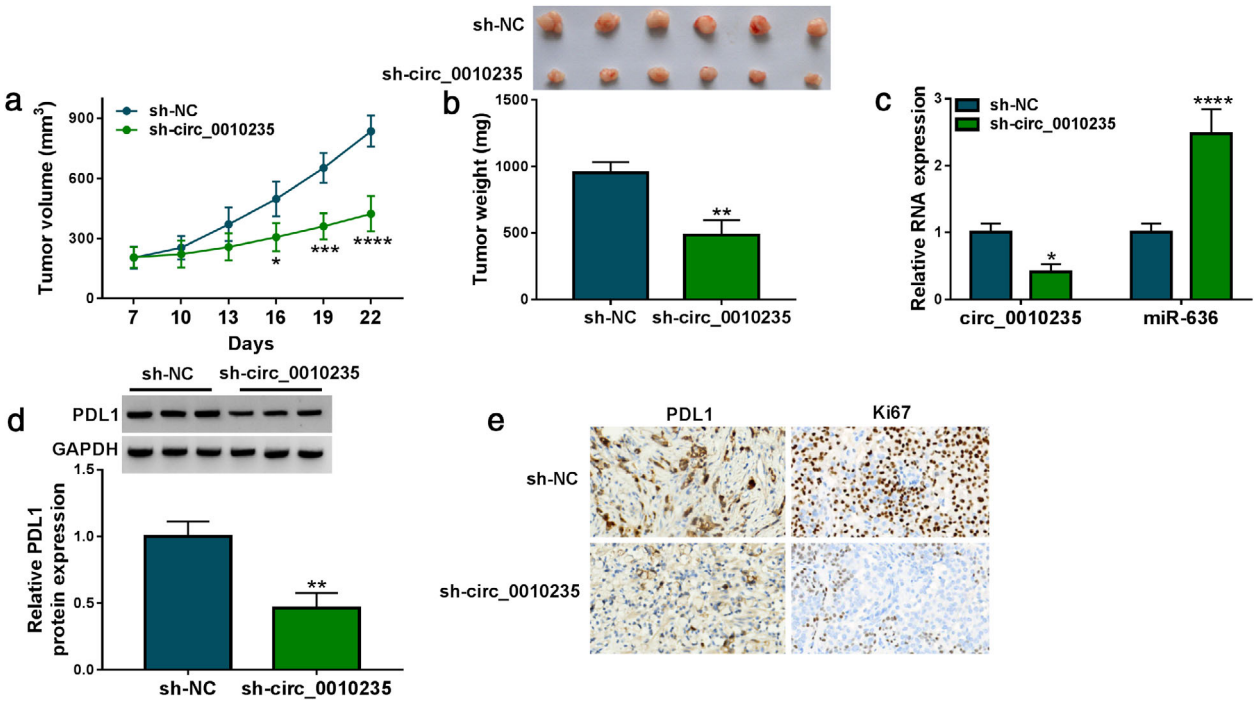

FIGURE 8 Circ_0010235 depletion blocked tumor growth in vivo. A549 cells were transfected with sh-NC or sh-circ_0010235 and then injected into the mice. (a) Tumor volume of nude mice was recorded every three days. (b) Tumor weight was measured after injection for 22 days. (c) The levels of circ_0010235 and miR-636 in tumor tissues were detected by qRT-PCR. (d) Western blot assay was used to examine the protein expression of PDL1 in tumor tissues. (e) IHC analysis was used to detect the expression of PDL1 and Ki67 in tumor tissues. $^{*}p < 0.05$, $^{**}p < 0.01$, $^{***}p < 0.001$, $^{****}p < 0.0001$

PDL1 protein expression caused by miR-636 in A549 and H1299 cells (Figure 6a). Moreover, restoration of miR-636 inhibited cell viability, colony formation ability, and DNA synthesis, while these effects were abrogated by upregulating PDL1 in A549 and H1299 cells (Figures 6b–d). Additionally, miR-636 overexpression increased cell apoptosis and inhibited cell invasion, CyclinD1 and MMP9 protein levels, which could be reversed by increasing PDL1 in A549 and H1299 cells (Figure 6e–h). Furthermore, enforced expression of miR-636 enhanced IFN-γ and TNF-α levels and decreased survival rate, which were neutralized by overexpression of PDL1 in A549 and H1299 cells (Figure 6i–k). In conclusion, miR-636 exerted an anticancer role in lung cancer cells by targeting PDL1.

Circ_0010235 positively regulated PDL1 expression by sponging miR-636

To explore whether circ_0010235 sponged miR-636 to regulate PDL1 expression, A549 and H1299 cells were transfected with si-NC, si-circ_0010235, si-circ_0010235 + anti-miR-NC, or si-circ_0010235 + anti-miR-636. As shown in Figures 7a,b, circ_0010235 knockdown decreased the protein expression of PDL1, which was reversed by inhibition of miR-636, indicating that circ_0010235 positively regulated PDL1 expression by acting as a miR-636 sponge.

Knockdown of circ_0010235 reduced tumor growth in vivo

A mice xenograft model was established to assess whether circ_0010235 acted as a tumor promoter in vivo. In comparison with the sh-NC group, tumor volume and weight were markedly reduced in the sh-circ_0010235 group (Figure 8a, b). In agreement with the in vitro results, circ_0010235 downregulation reduced circ_0010235 expression and PDL1 protein expression as well as enhancing miR-636 expression in tumor tissues (Figure 8c,d). IHC analysis showed that circ_0010235 interference suppressed PDL1 and Ki67 (a proliferation marker) expression in excised tumor masses (Figure 8e). The above results indicated that circ_0010235 knockdown repressed tumor growth in vivo via increasing miR-636 and decreasing PDL1 expression.

DISCUSSION

Lung cancer is a common malignant tumor, accounting for about 13% of total cancer diagnoses.[20] In our study, we demonstrated that circ_0010235 knockdown repressed the growth and invasion and enhanced apoptosis and antitumor immunity in lung cancer cell lines by sponging miR-636 and regulating PDL1.

CircRNAs are considered as key regulators in diverse cellular processes.[21] Increasing evidence has shown that many circRNAs (such as circ_010763, circ_001010, and circ_0078767) can affect lung cancer progression.[22–24] As a circRNA, circ_0010235 has previously been found to be overexpressed in lung cancer cells and tissues, and depletion of circ_0010235 limited the proliferation and autophagy and contributed to apoptosis in lung cancer cell lines through regulation of miR-433-3p/TIPRL axis.[13] In line with this research, an increase of circ_0010235 expression was also found in lung cancer cells and tissues, and circ_0010235 silencing repressed lung cancers cell growth and invasion and induced cell apoptosis. IFN-γ and TNF-α have been reported to have many antitumor effects, such as blocking angiogenesis, directly inhibiting tumor growth, or stimulating macrophages.[25] CIK cells can not only kill tumor cells directly, but also secrete a variety of cytokines (including IL-2, TNF-α and IFN-γ), which increases the systemic antitumor immunity. Here, we found that circ_0010235 knockdown increased antitumor immune response by increasing IFN-γ and TNF-α levels and CIK cell cytotoxicity against lung cancer cells. These results suggest that circ_0010235 could regulate lung cancer cell behaviors and antitumor immunity.

CircRNAs are involved in the development of many malignancies via serving as sponges of miRNAs and protecting the genes that are targeted by miRNAs.[26] Next, we searched the potential targets of circ_0010235 and validated that miR-636 was directly targeted by circ_0010235. MiR-636 plays a tumor-promoting or tumor-suppressing role in different cancer, acting as a tumor inhibitor in cervical cancer and ovarian cancer[27,28] and a promoter in bladder cancer.[29] In lung cancer, interference of circ_100876 suppressed lung cancer progression via regulating miR-636/RET axis.[30] Nevertheless, the exact function of miR-636 in lung cancer has not been fully clarified. Herein, a low level of miR-636 in lung cancer cells and tissues was observed. MiR-636 reduction could reverse the effects of circ_0010235 deficiency on inhibiting lung cancer cell progression and increase the antitumor immune response, suggesting that circ_0010235 exerts its role in lung cancer by sponging miR-636.

MiRNAs can directly bind to target mRNAs to exert their roles in many diseases.[31] According to bioinformatics tool and experimental verification, PDL1 has been demonstrated to be targeted by miR-636. PDL1, a 40-kDa transmembrane protein, is considered be a key "do not find me" signal for the adaptive immune system.[32] PDL1 has been reported to be overexpressed in many cancers and can bind with programmed cell death protein 1 (PD1) to suppress the immune system.[33,34] These findings indicate that PDL1 can promote immune escape of tumor cells and might be an immunotherapy target for lung cancer. In addition, PDL1 was found to be upregulated in lung cancer tissue samples, and involved in lung cancer progression and tumor immune escape in lung cancer cells.[35,36] In our study, PDL1 was also observed to be upregulated in lung cancer. Moreover, PDL1 upregulation abated the function of miR-636 in inhibiting lung cancer cell progression and increased antitumor immunity, revealing the promoting role of PDL1 in lung cancer and immune escape. Furthermore, circ_0010235 can regulate PDL1 expression via sponging miR-636 in lung cancer cells. Consistent with in vitro results, circ_0010235 interference could also block tumorigenesis in vivo by modulation of the miR-636/PDL1 axis. However, there are some limitations and shortcomings in this study. First, A549 and H1299 cells are only two lung cancer cell lines, which cannot evaluate the entire lung cancer. Second, one gene may be regulated and targeted by many molecules; other circRNA/miRNAs might also contribute to lung cancer development through regulating PDL1.

In conclusion, in this study, circ_0010235 was highly expressed in lung cancer, and circ_0010235 accelerated lung cancer progression and immune escape by sponging miR-636 and upregulating PDL1. Our research may provide a novel molecular mechanism for lung cancer development

and offer a promising target for immune therapy in the future.

CONFLICT OF INTEREST

The authors declare that they have no conflict of interest.

ORCID

Yongsheng Li https://orcid.org/0000-0002-2156-6439

REFERENCES

1. Bray F, Ferlay J, Soerjomataram I, Siegel RL, Torre LA, Jemal A. Global cancer statistics 2018: GLOBOCAN estimates of incidence and mortality worldwide for 36 cancers in 185 countries. CA Cancer J Clin. 2018;68:394–424.
2. Siegel R, Naishadham D, Jemal A. Cancer statistics, 2012. CA Cancer J Clin. 2012;62:10–29.
3. Hirsch FR, Suda K, Wiens J, Bunn PA Jr. New and emerging targeted treatments in advanced non-small-cell lung cancer. Lancet. 2016;388:1012–24.
4. Jiang J, Wu C, Lu B. Cytokine-induced killer cells promote antitumor immunity. J Transl Med. 2013;11:83.
5. Edinger M, Cao YA, Verneris MR, Bachmann MH, Contag CH, Negrin RS. Revealing lymphoma growth and the efficacy of immune cell therapies using in vivo bioluminescence imaging. Blood. 2003;101:640–8.
6. Liu J, Liu T, Wang X, He A. Circles reshaping the RNA world: from waste to treasure. Mol Cancer. 2017;16:58.
7. Chen LL. The biogenesis and emerging roles of circular RNAs. Nat Rev Mol Cell Biol. 2016;17:205–11.
8. Shang Q, Yang Z, Jia R, Ge S. The novel roles of circRNAs in human cancer. Mol Cancer. 2019;18:6.
9. Zhang Z, Yang T, Xiao J. Circular RNAs: promising biomarkers for human diseases. EBioMedicine. 2018;34:267–74.
10. Patop IL, Kadener S. circRNAs in cancer. Curr Opin Genet Dev. 2018;48:121–7.
11. Yang H, Zhao M, Zhao L, Li P, Duan Y, Li G. CircRNA BIRC6 promotes non-small cell lung cancer cell progression by sponging microRNA-145. Cell Oncol (Dordrecht). 2020;43:477–88.
12. Zhang N, Nan A, Chen L, Li X, Jia Y, Qiu M, et al. Circular RNA circSATB2 promotes progression of non-small cell lung cancer cells. Mol Cancer. 2020;19:101.
13. Zhang F, Cheng R, Li P, Lu C, Zhang G. Hsa_circ_0010235 functions as an oncogenic drive in non-small cell lung cancer by modulating miR-433-3p/TIPRL axis. Cancer Cell Int. 2021;21:73.
14. Bach DH, Lee SK, Sood AK. Circular RNAs in cancer. Mol Ther Nucleic Acids. 2019;16:118–29.
15. Gattolliat CH, Uguen A, Pesson M, Trillet K, Simon B, Doucet L, et al. MicroRNA and targeted mRNA expression profiling analysis in human colorectal adenomas and adenocarcinomas. Eur J Cancer. 2015;51:409–20.
16. Jiang X, Wang J, Deng X, Xiong F, Ge J, Xiang B, et al. Role of the tumor microenvironment in PD-L1/PD-1-mediated tumor immune escape. Mol Cancer. 2019;18:10.
17. Hong W, Xue M, Jiang J, Zhang Y, Gao X. Circular RNA circ-CPA4/let-7 miRNA/PD-L1 axis regulates cell growth, stemness, drug resistance and immune evasion in non-small cell lung cancer (NSCLC). J Exp Clin Cancer Res. 2020;39:149.
18. Schmidt-Wolf GD, Negrin RS, Schmidt-Wolf IG. Activated T cells and cytokine-induced CD3+CD56+ killer cells. Ann Hematol. 1997;74:51–6.
19. Haque S, Harries LW. Circular RNAs (circRNAs) in health and disease. Genes. 2017;8:353.
20. Torre LA, Bray F, Siegel RL, Ferlay J, Lortet-Tieulent J, Jemal A. Global cancer statistics, 2012. CA Cancer J Clin. 2015;65:87–108.
21. Wang Y, Mo Y, Gong Z, Yang X, Yang M, Zhang S, et al. Circular RNAs in human cancer. Mol Cancer. 2017;16:25.
22. Zhang P, Xue XF, Ling XY, Yang Q, Yu Y, Xiao J, et al. CircRNA_010763 promotes growth and invasion of lung cancer through serving as a molecular sponge of miR-715 to induce c-Myc expression. Eur Rev Med Pharmacol Sci. 2020;24:7310–9.
23. Wang Q, Kang PM. CircRNA_001010 adsorbs miR-5112 in a sponge form to promote proliferation and metastasis of non-small cell lung cancer (NSCLC). Eur Rev Med Pharmacol Sci. 2020;24:4271–80.
24. Chen T, Yang Z, Liu C, Wang L, Yang J, Chen L, et al. Circ_0078767 suppresses non-small-cell lung cancer by protecting RASSF1A expression via sponging miR-330-3p. Cell Prolif. 2019;52:e12548.
25. Olioso P, Giancola R, Di Riti M, Contento A, Accorsi P, Iacone A. Immunotherapy with cytokine induced killer cells in solid and hematopoietic tumours: a pilot clinical trial. Hematol Oncol. 2009;27:130–9.
26. Hansen TB, Jensen TI, Clausen BH, Bramsen JB, Finsen B, Damgaard CK, et al. Natural RNA circles function as efficient microRNA sponges. Nature. 2013;495:384–8.
27. Hu QL, Xu ZP, Lan YF, Li B. miR-636 represses cell survival by targeting CDK6/Bcl-2 in cervical cancer. Kaohsiung J Med Sci. 2020;36:328–35.
28. Ma J, Zhou C, Chen X. miR-636 inhibits EMT, cell proliferation and cell cycle of ovarian cancer by directly targeting transcription factor Gli2 involved in hedgehog pathway. Cancer Cell Int. 2021;21:64.
29. He Q, Huang L, Yan D, Bi J, Yang M, Huang J, et al. CircPTPRA acts as a tumor suppressor in bladder cancer by sponging miR-636 and upregulating KLF9. Aging. 2019;11:11314–28.
30. Song J, Shi W, Gao Z, Liu X, Wang W. Downregulation of circRNA_100876 inhibited progression of NSCLC in vitro via targeting miR-636. Technol Cancer Res Treat. 2020;19. https://doi.org/10.1177/1533033820951817
31. Felekkis K, Touvana E, Stefanou C, Deltas C. microRNAs: a newly described class of encoded molecules that play a role in health and disease. Hippokratia. 2010;14:236–40.
32. Ohaegbulam KC, Assal A, Lazar-Molnar E, Yao Y, Zang X. Human cancer immunotherapy with antibodies to the PD-1 and PD-L1 pathway. Trends Mol Med. 2015;21:24–33.
33. Shi L, Chen S, Yang L, Li Y. The role of PD-1 and PD-L1 in T-cell immune suppression in patients with hematological malignancies. J Hematol Oncol. 2013;6:74.
34. Bersanelli M, Buti S. From targeting the tumor to targeting the immune system: transversal challenges in oncology with the inhibition of the PD-1/PD-L1 axis. World J Clin Oncol. 2017;8:37–53.
35. Wei S, Wang K, Huang X, Zhao Z, Zhao Z. LncRNA MALAT1 contributes to non-small cell lung cancer progression via modulating miR-200a-3p/programmed death-ligand 1 axis. Int J Immunopathol Pharmacol. 2019;33:2058738419859699.
36. Wang J, Zhao X, Wang Y, Ren FH, Sun DW, Yan YB, et al. circRNA-002178 act as a ceRNA to promote PDL1/PD1 expression in lung adenocarcinoma. Cell Death Dis. 2020;11:32.

SUPPORTING INFORMATION

Additional supporting information may be found in the online version of the article at the publisher's website.

How to cite this article: Zhao J, Yan W, Huang W, Li Y. Circ_0010235 facilitates lung cancer development and immune escape by regulating miR-636/PDL1 axis. Thorac Cancer. 2022;13:965–76. https://doi.org/10.1111/1759-7714.14338